Journal of Experimental Botany, Vol. 70, No. 20 pp. 5631–5642, 2019
doi:10.1093/jxb/erz349 Advance Access Publication July 30, 2019
This paper is available online free of all access charges (see https://academic.oup.com/jxb/pages/openaccess for further details)

RESEARCH PAPER

Phosphate acquisition efficiency in wheat is related to root:shoot ratio, strigolactone levels, and PHO2 regulation

Pedro M. de Souza Campos[1,2,3,4,], Pablo Cornejo[2,4], Carlos Rial[6,], Fernando Borie[2,4,5], Rosa M. Varela[6], Alex Seguel[2,4,*] and Juan Antonio López-Ráez[3,*,]

[1] Programa de Doctorado en Ciencias de Recursos Naturales, Universidad de La Frontera, Temuco, Chile
[2] Centro de Investigación en Micorrizas y Sustentabilidad Agroambiental (CIMYSA-UFRO), Universidad de La Frontera, Temuco, Chile
[3] Department of Soil Microbiology and Symbiotic Systems, Estación Experimental del Zaidín (EEZ-CSIC), Granada, Spain
[4] Scientific and Technological Bioresource Nucleus (BIOREN-UFRO), Universidad de La Frontera, Temuco, Chile
[5] Departamento de Ciencias Agropecuarias y Acuícolas, Universidad Católica de Temuco, Temuco, Chile
[6] Allelopathy Group, Department of Organic Chemistry, Institute of Biomolecules (INBIO), Campus de Excelencia Internacional (ceiA3), School of Science, University of Cadiz, Spain

* Correspondence: alex.seguel@ufrontera.cl or juan.lopezraez@eez.csic.es

Received 10 December 2018; Editorial decision 17 July 2019; Accepted 18 July 2019

Editor: Ramanjulu Sunkar, Oklahoma State University, USA

Abstract

Inorganic phosphorus (Pi) fertilizers are expected to become scarce in the near future; so, breeding for improved Pi acquisition-related root traits would decrease the need for fertilizer application. This work aimed to decipher the physiological and molecular mechanisms underlying the differences between two commercial wheat cultivars (Crac and Tukan) with contrasting Pi acquisition efficiencies (PAE). For that, four independent experiments with different growth conditions were conducted. When grown under non-limiting Pi conditions, both cultivars performed similarly. Crac was less affected by Pi starvation than Tukan, presenting higher biomass production, and an enhanced root development, root:shoot ratio, and root efficiency for Pi uptake under this condition. Higher PAE in Crac correlated with enhanced expression of the Pi transporter genes *TaPht1;2* and *TaPht1;10*. Crac also presented a faster and higher modulation of the *IPS1*–miR399–*PHO2* pathway upon Pi starvation. Interestingly, Crac showed increased levels of strigolactones, suggesting a direct relationship between this phytohormone and plant P responses. Based on these findings, we propose that higher PAE of the cultivar Crac is associated with an improved P signalling through a fine-tuning modulation of *PHO2* activity, which seems to be regulated by strigolactones. This knowledge will help to develop new strategies for improved plant performance under P stress conditions.

Keywords: P signalling, phosphate starvation responses, phosphate transporters, root traits, strigolactones, wheat.

Introduction

Phosphorus (P) is the second most limiting nutrient in plants besides nitrogen, being involved in numerous cellular processes such as protein activation, energy transfer, signalling, and regulation of carbon metabolism (Lan *et al.*, 2015; Xu *et al.*, 2018). However, unlike nitrogen, which can be fixed by microorganisms, the amount of P available for agriculture is finite (Bovill *et al.*, 2013). Moreover, when compared with other essential macronutrients, P is one of the less abundant

elements in the lithosphere (0.1% of the total), highlighting the need for supplying P fertilizers to sustain modern agricultural production (Campos *et al.*, 2018). As a consequence, consumption of P fertilizers has increased worldwide in the past decades. P fertilizers are made from non-renewable resources such as rock phosphates, which are expected to become scarce in the near future as few mining sites are discovered and demand is expected to increase further by 50–100% in the next 30 years (Cordell *et al.*, 2009; Ulrich and Frossard, 2014). P is present in plants either as organic phosphate esters or as the free inorganic orthophosphate form (Pi). Remarkably, Pi has high affinity for both soil mineral particles and organic matter; therefore, its availability in agroecosystems is generally below a plant's demand, even in fertilized sites, where up to ~90% of the applied P fertilizer is not taken up by the roots in the first year (Syers *et al.*, 2008; López-Arredondo *et al.*, 2014). Therefore, although a huge amount of P fertilizers are used, plants are normally subjected to stress due to the low availability of this essential nutrient. Nevertheless, when P fertilization exceeds soil holding capacity, environmental problems associated with eutrophication due to P leaching are likely to occur (Bennett *et al.*, 2001). In addition, these fertilizers can contain heavy metals, such as cadmium, that may accumulate in arable soils as a result of the addition of rock phosphate (van de Wiel *et al.*, 2016).

Plants have developed an array of complex regulatory mechanisms to adapt themselves to low Pi availability in the soil, known as P starvation responses (PSRs), aiming to optimize its external and internal use (Puga *et al.*, 2017; Ham *et al.*, 2018). These responses include changes at genetic, biochemical, physiological, morphological, and rhizospheric levels (Puga *et al.*, 2017). PSRs include alterations in shoot and root morphology, growth and development, exudation of low molecular weight organic acid anions and Pi-releasing enzymes, modifications in lipids and carbohydrate metabolism, association with soil microorganisms, as well as the regulation of expression and activity of high-affinity Pi transporters (PHTs) (Lambers *et al.*, 2015; Campos *et al.*, 2018). Nevertheless, in order to respond accurately, plants need first to sense the P status both locally and systemically in order to orchestrate the appropriate responses (Lan *et al.*, 2015; Scheible and Rojas-Triana, 2015). PSRs are themselves complex, with a large set of genes (>1000) being regulated. However, new genomic findings have contributed to shed light on some mechanisms of P sensing, signalling, and homeostasis, especially in the model plants *Arabidopsis thaliana* and rice (*Oryza sativa*) (Liu *et al.*, 2012; Lan *et al.*, 2015). It is well established that the transcriptional activator *PHOSPHATE STARVATION RESPONSE 1* (*PHR1*) in Arabidopsis and its orthologous *OsPHR2* in rice play a key role in regulating the expression of numerous Pi starvation-induced (PSI) genes (Rubio *et al.*, 2001; Zhou *et al.*, 2008). Among them, special attention has been paid to the miRNA miR399, whose expression is highly induced by Pi deprivation (Pant *et al.*, 2008). This regulator has been shown to be a key systemic cue between plant tissues by modulating the activity of *PHO2*, which encodes a ubiquitin-conjugating E2 enzyme (UBC24) implicated in protein degradation (Lin *et al.*, 2008). Down-regulation of *PHO2* prevents the degradation of the Pi transporter PHO1, involved in Pi xylem loading, and some transporters of the PHT1 family, associated with Pi acquisition and translocation within the plant (Liu *et al.*, 2012; Huang *et al.*, 2013). Another key PSI gene family involved in P signalling and homeostasis is *At4/IPS1* in Arabidopsis and rice, respectively. These genes affect the miR399–*PHO2* interaction by sequestering free miR399 through a target mimicry mechanism, preventing its binding to *PHO2* transcripts and, thus, its degradation (Fig. 1) (Franco-Zorrilla *et al.*, 2007). Therefore, Pi acquisition and distribution within the plant are regulated mainly by the interaction of the triad *IPS1*–miR399–*PHO2*, which serves to fine-tune PSRs (Fig. 1).

Wheat (*Triticum aestivum* L.) is one of the most important food crops in the world, with global grain production of 7.5×10^{14} g in 2016, making it the third most harvested crop worldwide, after sugarcane (*Saccharum* spp.) and maize (*Zea mays* L.) (FAO, http://faostat3.fao.org/home/E). However, wheat production is highly dependent on P fertilizers, leading to a higher consumption per area when compared with other major crops (Heffer, 2013). Therefore, improving P fertilization efficiency in wheat cropping is a major goal in order to achieve a more sustainable agricultural production. The last can be achieved by improving the availability of P fertilizers in soil, such as by avoiding Pi sorption to soil particles, and/or by the development of P use-/acquisition-efficient plants (Campos *et al.*, 2018). While the first option increases operational costs and requires modern technology, often not accessible for producers, breeding for Pi acquisition-efficient root systems would provide benefits to both high- and low-input systems (Wissuwa *et al.*, 2001; Rose and Wissuwa, 2012). In recent years, some molecular mechanisms underlying P signalling and homeostasis in wheat have been revealed. Wang and co-workers characterized *TaPHR1*, and showed that overexpressing lines had improved root system architecture, enhanced Pi uptake, and higher yield (Wang *et al.*, 2013). In another breakthrough, the *IPS1*–miR399–*PHO2* system was shown to be functional in

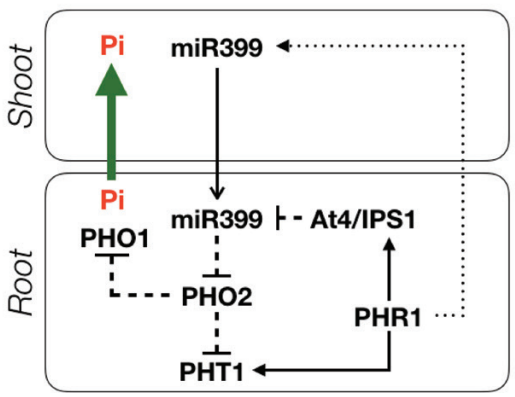

Fig. 1. Schematic summary of the P signalling and homeostasis pathway in plants. Upon Pi deficiency, expression of the miRNA miR399 is induced in the shoot. miR399 moves downwards, inactivating *PHO2* in the roots. Regulation of *PHO2* prevents the degradation of the Pi transporters *PHO1* and *PHT1*, which increase Pi uptake and translocation. Pi deficiency also induces the expression of *IPS1*, which binds miR399, modulating this response. Based on Puga *et al.* (2017). (This figure is available in colour at *JXB* online.)

wheat (Ouyang *et al.*, 2016). In that study, *TaPHO2* expression was found to be related to root and shoot growth, shoot Pi accumulation, and activity of some *PHT1* transporters (Ouyang *et al.*, 2016). In this context, the Pi transporter gene family *PHT1* from wheat has been recently identified, consisting of 16 phylogenetically distinct transporters (Grün *et al.*, 2017).

On the other hand, it is well known that phytohormones such as auxin, cytokinin, abscisic acid, ethylene, and in particular strigolactones (SLs) play synergistic roles in the regulation of P homeostasis when plants are subjected to P stress, through modulation of the P signalling- and homeostasis-associated pathways and ultimately root functioning (Waters *et al.*, 2017; Chien *et al.*, 2018). SLs are the latest class of phytohormones described, and have been shown to function as regulators of plant development/architecture and as signalling molecules in the rhizosphere to recruit arbuscular mycorrhizal fungi under Pi limitation (López-Ráez *et al.*, 2017; Waters *et al.*, 2017). Indeed, their biosynthesis is highly promoted under this stress condition (Yoneyama *et al.*, 2007, 2012; López-Ráez *et al.*, 2008). Recently, it has been shown that exogenous application of the synthetic SL analogue GR24 induced root hair elongation, anthocyanin accumulation, production of acid phosphatases, and reduced plant weight (Ito *et al.*, 2015), which are characteristic PSRs, suggesting a potential overlap between these two signalling and homeostasis pathways in plants. Although the molecular mechanisms that regulate P signalling and homeostasis, and their associated plant morphological changes and Pi uptake capacity, are being established at the laboratory level, only a few studies have verified these findings in commercial cultivars so far. In the present work, we aimed to characterize at the physiological and molecular level two commercial wheat cultivars—Crac and Tukan—with different Pi acquisition efficiencies, and to relate these phenotypes to their ability to regulate P signalling and homeostasis under Pi-limited conditions. The results provide new insights into the regulation of P signalling and homeostasis in plants and suggest new potential targets for future breeding strategies in plant production.

Materials and methods

Plant material and growth conditions

Seeds from the wheat cultivars Crac and Tukan (formerly know as TCRB14 and STKI14, respectively) were surface-sterilized in 4% sodium hypochlorite, rinsed thoroughly with sterile distilled water, and germinated for 72 h on moistened filter paper at 25 °C in darkness. Precise phenotyping for optimal root system characteristics is difficult and time-consuming as root traits are hidden under the soil, making their extraction for observation difficult (Zhu *et al.*, 2011). Therefore, different 'artificial' growing methods are used under laboratory conditions to facilitate their access, such as growing plants in liquid culture (hydroponics) or in transparent surfaces (rhizoboxes). These methods, although they do not fully represent the root growth in soil, give valuable clues to understand general features, and the physiological and genetic background behind them (Hargreaves *et al.*, 2009). In order to access the effects of Pi deficiency on plant development and Pi acquisition of these cultivars, seedlings of each genotype were grown hydroponically (Supplementary Fig. S1a at *JXB* online) for 2 weeks with a standard nutrient solution (Taylor and Foy, 1985) containing 200 μM Pi in 1 litre containers and then half of the plants were submitted to Pi starvation (10 μM Pi in nutrient solution) for 3 weeks. In parallel, seedlings of each genotype were transferred to 0.5 litre plastic pots with a mixture of autoclaved substrate of sand and vermiculite (1:1) and were watered manually with standard nutrient solution low in Pi (10 μM) for 33 d (Supplementary Fig. S1b). In addition to the experiments previously mentioned, another set of plants were grown for 8 weeks in rhizoboxes (30 cm height, 20 cm width, and 0.7 cm depth) filled with an acidic high P-fixing soil without P fertilization (Supplementary Table S1; Supplementary Fig. S2a). Plants were grown under greenhouse conditions with temperatures ranging from 16 °C to 23 °C during the day and from 10 °C to 18 °C at night, and were harvested at Zadoks growth stage 23 (Zadoks *et al.*, 1974).

For gene expression analysis and SL quantification, six seedlings of each cultivar were grown hydroponically in 3 litre containers, containing a modified Long Ashton nutrient solution with 150 μM Pi (Hewitt, 1966) in a greenhouse for a total of 5 weeks (Supplementary Fig. S1c). Nutrient solution was replaced twice a week. After 4 weeks, half of the plants were transferred to a modified nutrient solution without P and were left to grow for another week. For the time course Pi starvation experiment, plants were grown for 4 weeks under normal P conditions, and then half of the plants were subjected to 2, 4, and 7 d Pi deprivation. Six independent plants were grown per treatment and time point. Shoots, roots, and root exudates were collected, weighed, frozen with liquid nitrogen, and kept at –80 °C until use.

Root architecture measurements

For the phenotyping experiments, root systems were cleaned after harvest, arranged to minimize overlaps (Yao *et al.*, 2009), placed in an A3-sized Perspex tray filled with water, and scanned in both grey-scale and colour in a Epson Expression 11000XL calibrated for Image Analysis. The images were then subjected to software analysis (WinRhizo; Regent Instruments, Quebec, Canada), and root length, specific area, and average diameter were assessed.

Pi acquisition

After root architecture determination, plants were separated into roots and shoots, and both parts were weighed and dried at 65 °C in a forced-air oven for 72 h. After drying, the root and shoot samples were weighed, crushed, ground, ashed in a furnace at 550 °C, and digested using an H_2O:HCl:HNO_3 mixture (8:1:1, v/v/v). Then, Pi content was determined using the vanadate–molybdate colorimetric method (Murphy and Riley, 1962).

RNA extraction and gene expression analysis by qPCR

Total RNA from roots was extracted using TRIsure™ (Bioline, Toronto, Canada) according to the manufacturer's instructions. The RNA was treated with RQ1 DNase (Promega, Madison, WI, USA) and purified through a silica column using the RNA Clean & Concentrator™ (Zymo Research, irvine, CA, USA). Before storage at –80 °C, RNA was quantified using a Nanodrop 2000C spectrophotometer (Thermo Scientific, Wilmington, DE, USA) and its integrity checked by gel electrophoresis. The first-strand cDNA was synthesized with 1 μg of purified total RNA using the PrimeScript™ RT Master Mix (Clontech, Fremont, CA, USA) according to the manufacturer's instructions. The expression of marker genes for different P signalling and homeostasis pathways (Supplementary Table S1) was analysed by real-time quantitative PCR (qPCR). All reactions were performed using TB Green™ Premix Ex Taq™ (Kusatsu, Shiga, Japan) on an iCycler iQ5 system (Bio-Rad), with 5 μl of single-stranded cDNA (diluted 1:50) and specific primers for each gene, except for *TaPht1;10* and tae-miR399b, where a dilution of 1:5 was used. In the case of the gene *TaPht1:2*, it is present in chromosomes A and B, showing high sequence similarities among them; therefore, it was not possible to design specific primers able to differentiate the expression of the two alleles (Grün *et al.*, 2017). The amplification protocol included an initial denaturation at 95 °C for 3 min followed by 35 cycles of 95 °C for 30 s, 58 °C for 30 s, and 72 °C for 30 s. The specificity of the different amplicons was checked by a melting curve analysis (from 65 °C to 100 °C) at the end of the amplification protocol. Five independent biological replicates were analysed per treatment and time point, and each

PCR was done in duplicate. Relative quantification of specific mRNA levels was performed using the comparative $2^{-\Delta Ct}$ method. Expression values were normalized using the housekeeping gene *TahnRNPQ* (Grün *et al.*, 2017).

Strigolactone quantification

Germination bioassays were performed using extracts from frozen roots from plants grown for molecular analysis. For SL extraction, root extracts were processed as described by López-Ráez *et al.* (2008). SLs are germination stimulants of root parasitic plants of the family Orobancheaceae (Bouwmeester *et al.*, 2007; López-Ráez *et al.*, 2017). Therefore, germination assays with seeds of these parasitic weeds is an indirect way to estimate SL levels. Germination bioassays with pre-conditioned seeds of the parasitic plants *Phelipanche ramosa* were performed as described by López-Ráez *et al.* (2008). The synthetic SL analogue 2-*epi*-GR24 and demineralized water were included as positive and negative controls, respectively. Extract dilutions of 1:10 and 1:20 were tested for seed germination. After 7 d, the germinated and non-germinated seeds were counted using a binocular loupe. In addition to the germination bioassays, SLs were quantified by UHPLC-MS/MS using GR24 as internal standard as described by Rial *et al.* (2019). Briefly, 0.1 g of ground root material was extracted with 1 ml of ethyl acetate in an ultrasonic bath for 10 min, centrifuged for 10 min at 5000 rpm, concentrated in a rotary evaporator, and stored at –80 °C. Before the chromatographic analysis, extracts were dissolved with MeOH (1:1, v/v), and GR24 was added to each sample to a final concentration of 10 µg l^{-1}. Chromatographic analyses were carried in a Bruker EVOQ Triple Quadrupole Mass Spectrometer with an electrospray ionization (ESI) source in positive mode. The mobile phase consisted of solvent A (water, 0.1% formic acid) and solvent B (MeOH, 0.1% formic acid) and the flow rate was set to 0.3 ml min^{-1}. The optimized linear gradient system was as follow: 0–0.5 min, 50% B; 0.5–5 min, to 100% B; 5–7 min, 100% B; 7–7.5 min, to 50% B; 7.5–10.5 min, 50% B. The injection volume was 5 µl. The instrument parameters were set as described by Rial *et al.* (2019)

Statistical analysis

Means for plant growth, root architecture measurements, Pi acquisition, gene expression analysis by qPCR, and SL production were obtained from the results of five replicates. Data were assessed for normality, transformed when necessary, and significant differences between means were analysed by independent Student's *t*-test or ANOVA followed by Tukey LSD when suited. Correlations among the different variables were performed using the *r* Pearson coefficient. All statistical analyses were carried out with R software.

Results

Pi acquisition and root system architecture in Crac and Tukan

In acidic soils, including Andisols in Chile, Pi bioavailability is rather low, many times due to high levels of iron and aluminium, which greatly affects plant productivity. In a previous study, a screening of wheat cultivars commonly used in Chile revealed high variations in Pi acquisition and grain yield when grown in high Pi-fixing Andisol (Seguel *et al.*, 2017). From that study, we selected two cultivars—Crac and Tukan—showing contrasting Pi acquisition efficiency (PAE) under Pi-deficient conditions. The most efficient cultivar, Crac, yielded almost three times more than the less efficient cultivar, Tukan, at low Pi fertilization levels (Seguel *et al.*, 2017). In the present work, we aim to decipher the physiological and molecular mechanisms behind such phenotypes. For that, plants of these two wheat cultivars were grown in different substrates and under different P conditions, and their Pi acquisition capacity compared. Similar results were obtained with the different growing conditions. When grown in hydroponics (Supplementary Fig. S1a) with sufficient Pi, both cultivars accumulated and allocated P in a similar manner to shoot and roots. Pi starvation reduced Pi uptake in both cultivars. However, despite the loss of Pi accumulation in both organs, the loss was significantly lower in Crac than in Tukan (Table 1; Supplementary Table S2). Indeed, Pi-starved Crac plants accumulated 25% and 17% more Pi in the shoots and in the roots, respectively, than the less efficient cultivar Tukan. Differences in Pi uptake between the two cultivars were even higher when using pots with inert substrate, where Crac accumulated 40% and 60% more Pi in shoots and roots, respectively, than Tukan (Table 1). The same pattern was also observed in soil-grown plants in rhizoboxes, although to a lesser extent (Supplementary Fig. S2b). Interestingly, despite the different Pi uptake capacities of the two cultivars under Pi limitation, no significant differences were observed in their root Pi concentration (Table 1), suggesting that the increased P accumulation in Crac was associated with a larger root system.

Table 1. *Phosphate (Pi) uptake, concentration, and root efficiency in accumulating Pi in shoots, roots, and the whole plant in Crac and Tukan*

Tissue	cv	Hydroponic (+P)			Hydroponic (–P)			Pot (-P)		
		P uptake (µg)	P concentration (mg g^{-1})	Root efficiency (mg P m^{-2})	P uptake (µg)	P concentration (mg g^{-1})	Root efficiency (mg P m^{-2})	P uptake (µg)	P concentration (mg g^{-1})	Root efficiency (mg P m^{-2})
Shoot	Crac	1060.±158	1.57±0.23	61.57±1.60	600±32*	1.18±0.09*	17.73±0.55	678±43**	1.06±0.04**	22.41±1.61*
	Tukan	1130±43	1.41±0.04	74.17±5.05	480±22	0.92±0.05	17.04±1.99	406±28	0.89±0.02	18.48±0.77
Roots	Crac	180±16	1.01±0.08	10.51±1.02	120±02*	0.44±0.03	03.65±0.11	120±18**	0.40±0.06	3.61±0.51*
	Tukan	180±24	1.12±0.14	11.94±1.31	100±06	0.51±0.03	03.76±0.23	46±5	0.30±0.02	2.28±0.16
Plant	Crac	1240±157	1.45±0.13	72.07±6.56	720±29**	0.92±0.01**	21.38±0.45	797±44***	0.88±0.04**	26.46±2.05*
	Tukan	1310±47	1.36±0.02	86.10±5.17	580±15	0.81±0.02	20.80±1.81	421±41	0.73±0.01	20.76±0.71

Plants were grown in Pi-sufficient conditions (+P; 200 µM, hydroponically) and under Pi starvation (–P; 10 µM, hydroponically and in pots) and were harvested at Zadoks growth stage 23 (Zadoks *et al.*, 1974).
Data represent the means of five independent replicates (±SE). Asterisks indicate the significance of differences between the cultivars in the same condition, as determined by Student's *t*-test analysis: *P<0.05, **P<0.01, ***P<0.001.

Shoot and root development under Pi deficiency

One of the main symptoms of Pi deficiency in plants is the enhanced root:shoot ratio; by either a reduction in shoot growth or an increase in root production, or both (Ericsson, 1995; Chien *et al.*, 2018). To ascertain whether the differences observed in PAE between Crac and Tukan are associated with plant development, their shoot and root architecture were analysed. As expected, no significant differences in growth were observed under normal Pi conditions when grown hydroponically (Fig. 2a). However, under Pi starvation, plants showed a clear reduction in shoot growth (P<0.01), with a concomitant increase of root production compared with plants growing under normal Pi conditions (Fig. 2a; Supplementary Table S3). The effect was more severe in the less efficient cultivar Tukan, with a 37% reduction in shoot biomass, while the reduction was only 23% in Crac. The opposite effect was observed in the roots, where an increase in biomass of 30% was found in Tukan under Pi starvation, while the increase was up to 59% in Crac (Fig. 2a; Supplementary Table S3). Taken together, hydroponically grown plants displayed an average increase of the root:shoot ratio of 128% and 87% for Crac and Tukan, respectively (Fig. 2b; Supplementary Table S3). The same trend was observed in plants grown in pots with substrate, where Crac showed more shoot (34%) and root (42%) biomass than Tukan under Pi starvation, giving rise to a 20% higher root:shoot ratio in Crac (Fig. 2b). A similar pattern was also observed in plants grown in soil (Supplementary Fig. S2d, e). Therefore, a positive correlation between Pi accumulation and root:shoot ratio (R^2=0.87, R^2=0.95, and R^2=0.85, P<0.01, for hydroponic, pot, and rhizobox experiments, respectively) under Pi starvation was observed in all growing conditions.

Additionally, parameters associated with root system architecture, such as total root length and root area, were evaluated (Fig. 3). In hydroponics, Pi deprivation increased root length in both cultivars by 113% and 80% in Crac and Tukan, respectively (Fig. 3a; Supplementary Table S3). Root surface area also increased under Pi starvation, by 98% and 73%, respectively (Fig. 3b; Supplementary Table S3). In the pot experiment, root

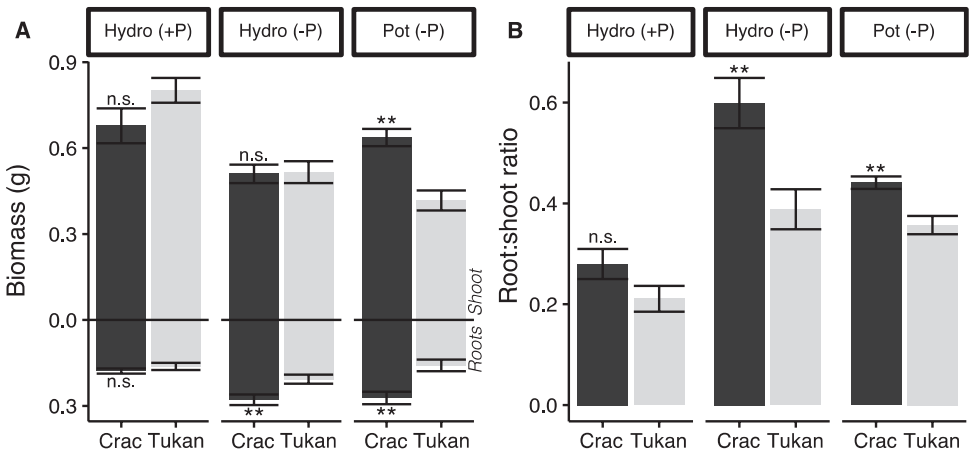

Fig. 2. Growth rate of wheat cultivars Crac (dark bars) and Tukan (light bars) in sufficient Pi conditions (+P; 200 μM, hydroponically) and under Pi starvation (–P; 10 μM, hydroponically and in pots) harvested at Zadoks growth stage 23 (Zadoks *et al.*, 1974). Graphics represent shoot and root biomass (A) and root:shoot ratio (B). Data represent the means of five independent replicates (±SE). n.s, non-significant differences. Asterisks indicate the significance of the differences between the cultivars in the same condition as determined by Student's *t*-test: **P<0.01.

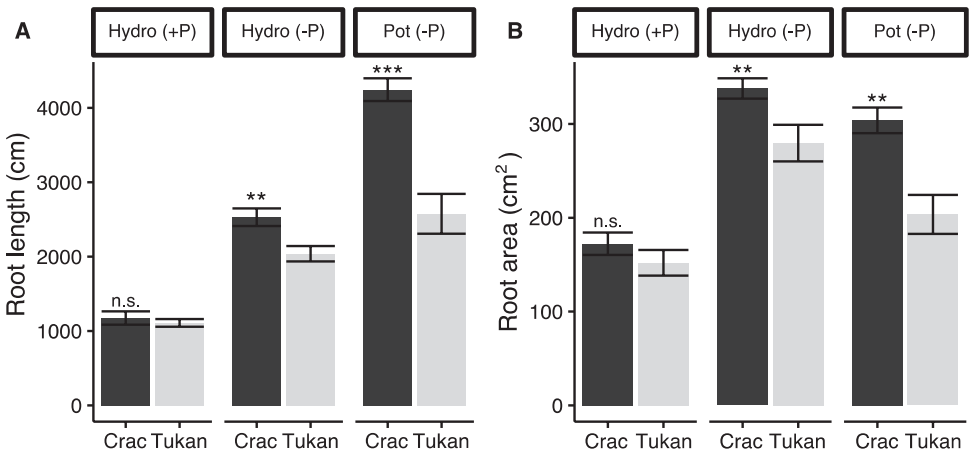

Fig. 3. Root system architecture of wheat cultivars Crac (dark bars) and Tukan (light bars) grown in sufficient Pi condition (+P; 200 μM, hydroponically) and under Pi starvation (–P; 10 μM, hydroponically and in pots) harvested at Zadoks growth stage 23 (Zadoks *et al.*, 1974). Graphics show total root length (A) and root surface area (B). Data represent the means of five independent replicates (±SE). n.s, non-significant differences. Asterisks indicate the significance of differences between the cultivars in the same condition as determined by Student's *t*-test: **P<0.01, ***P<0.001.

length (~65%) and surface area (~50%) were also greater in the most efficient cultivar, Crac, than in Tukan (Fig. 3). The same behaviour was observed in plants growing in rhizoboxes, with Crac showing wider root systems (Supplementary Fig. S2f, g). Differences in the diameter of the roots were also observed, roots of the cultivar Crac being significantly thinner (2.27 mm) than those of Tukan (2.41 mm) (P<0.01). These differences in average diameter were also detected in plants growing in rhizoboxes with soil (Supplementary Fig. S2h). In order to assess the root system efficiency in acquiring Pi, root efficiency (Pi uptake per root area) was calculated. Although few differences were observed among cultivars in the hydroponic experiment, the losses of efficiency from Pi-sufficient to Pi-deficient conditions in Tukan were significantly higher for all the experimental variables compared with those observed in Crac (Supplementary Table S3). Nevertheless, Crac plants growing in pots and rhizoboxes acquired significantly more Pi per root area compared with Tukan (Table 1; Supplementary Fig. S2i). Together, these results suggest a more developed and efficient root system for this genotype under P deficiency.

Gene expression of Pi transporters

We investigated whether the higher root efficiency observed for Crac was related to a higher induction of Pi transporters. For that, a new experiment under normal and Pi-deficient conditions was carried out in hydroponics, and gene expression levels of different Pi transporters were analysed by qPCR. Wheat has 16 phylogenetically distinct Pi transporters, seven of them being induced by Pi deprivation (Grün *et al.*, 2017). We analysed the expression profile of two of them, *TaPht1;2a/b* and *TaPht1;10*. The first one is the most hightly expressed, and it was described as a fast responsive Pi marker. The other shows low expression levels, and its expression is increased with time (Grün *et al.*, 2017). The remaining Pi-inducible *TaPHT1* shows similar expression patterns either to *TaPht1;2a/b* or to *TaPht1;10*, but with lower expression levels (Grün *et al.*, 2017; Teng *et al.*, 2017). For that reason, they were not analysed in this work. Expression analysis revealed major differences among the two cultivars and their responses to Pi deprivation, with Crac showing higher basal levels of both transporters. The expression of *TaPht1;2a/b* was ~140 times higher in Crac than in Tukan, and Pi starvation induced its expression levels 6- and 13-fold in Crac and Tukan, respectively (Fig. 4a). Therefore, the levels of *TaPht1;2a/b* upon Pi stress were ~50-fold higher in Crac. A similar pattern was observed for *TaPht1;10*, although its expression levels were much lower than that of *TaPht1;2a/b* (>70 times in Crac). In this case, basal transcripts levels of *TaPht1;10* in Crac were three times higher than in Tukan, and the induction by Pi deficiency was 10- and 2-fold in Crac and Tukan, respectively, giving rise to a 15-fold greater expression in the former under stress conditions (Fig. 4b).

Crac and Tukan show different regulation of P signalling and homeostasis

All adaptive responses that plants have evolved to cope with Pi deficiency are regulated through P signalling and homeostasis mechanisms, which begin with the integration of the information of the extracellular Pi concentration and its levels in the different organs (Puga *et al.*, 2017). Here, the *IPS1*-mediated signalling cascade, including *PHR1–IPS1*–miR399–*PHO2*, plays a pivotal role in P homeostasis regulation by coordinating the activities of Pi uptake and its root–shoot translocation through the transporters *PHT1s* and *PHO1* (Fig. 1) (Ouyang *et al.*, 2016; Ham *et al.*, 2018). To investigate whether Crac and Tukan presented differences in the P signalling and homeostasis pathway, we analysed the gene expression of *TaIPS1*, tae-miR399 [specifically from tae-miR399b family members, with confirmed expression and regulation activity in wheat roots under Pi starvation (Ouyang *et al.*, 2016)], *TaPHO2*, and *TaPHO1* in roots of the two cultivars after 7 d of Pi deprivation and under normal conditions. No differences in the transcript levels of *TaIPS1* were found under optimal Pi conditions, but a clear induction by Pi starvation was observed in both cultivars (Fig. 5a). Interestingly, a 10-fold higher induction was

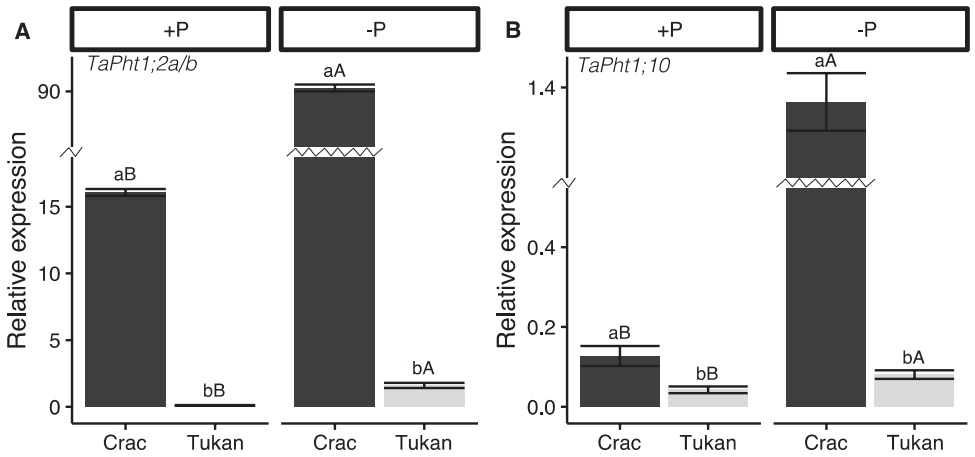

Fig. 4. Gene expression analysis of two *TaPHT1s* Pi transporters in roots of Crac (dark bars) and Tukan (light bars) plants grown in nutrient solution with Pi (+P; 150 μM) and without Pi for the last week (–P) harvested at Zadoks growth stage 24 (Zadoks *et al.*, 1974). Graphics represent expression of *TaPht1;2a/b* (A) and *TaPht1;10* (B). Expression levels were referenced to the expression of the housekeeping gene *TahnRNPQ*. Bars represent the means of five independent replicates (±SE). Lower case letters indicate differences between cultivars in the same condition, and upper case letters indicate differences within the same cultivar under normal and deficient Pi conditions as determined by Student's *t*-test analysis (P<0.05).

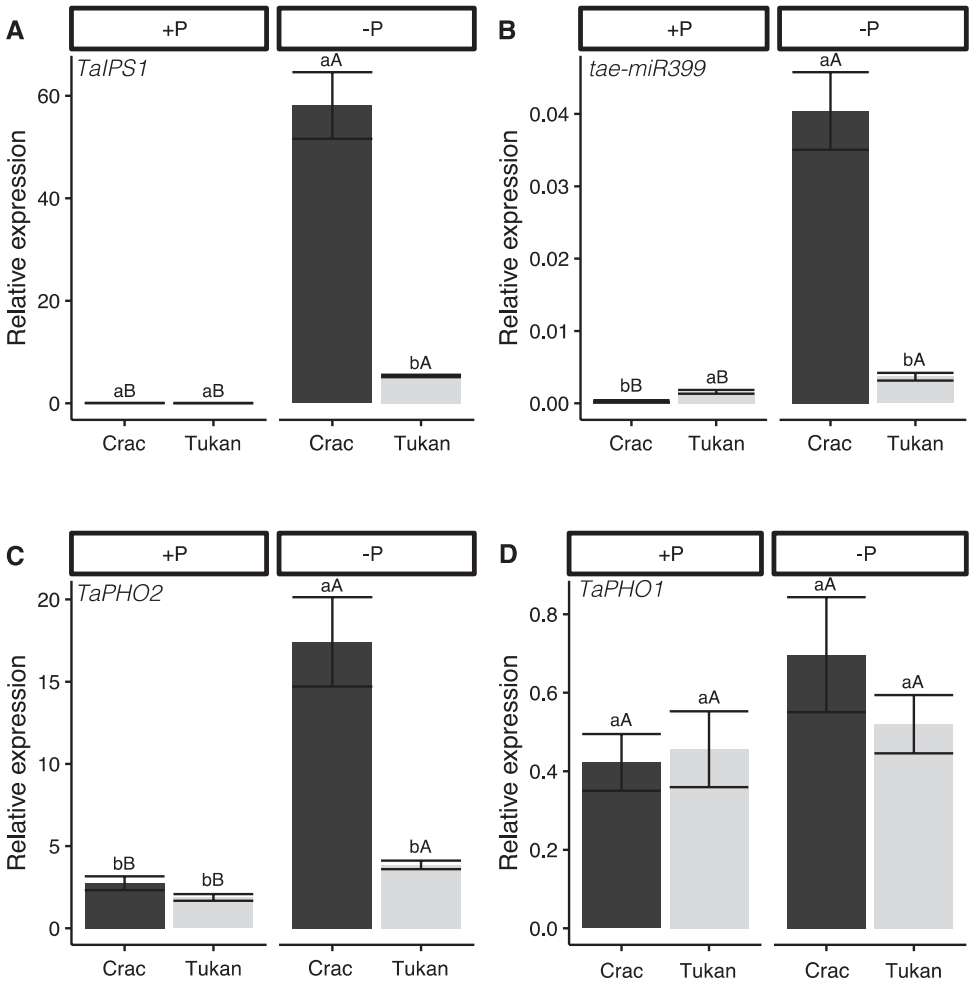

Fig. 5. Expression levels of genes involved in P signalling and homeostasis in roots of Crac (dark bars) and Tukan (light bars) plants grown in nutrient solution with Pi (+P; 150 μM) and without Pi for the last week (–P) harvested at Zadoks growth stage 24 (Zadoks *et al.*, 1974). Graphics represent gene expression of *TaIPS1* (A), tae-miR399 (B), *TaPHO2* (C), and *TaPHO1* (D). Expression levels were referenced to the expression of the housekeeping gene *TahnRNPQ*. Bars represent the means of five independent replicates (±SE). Lower case letters indicate differences between cultivars in the same condition, and upper case letters indicate differences within the same cultivar under normal and deficient Pi conditions, as determined by Student's *t*-test ($P<0.05$).

observed in Crac compared with Tukan. As for *TaIPS1*, Pi starvation promoted tae-miR399b expression in both cultivars, this increase being much higher in Crac (128-fold) than in Tukan (~2-fold). Thus, the number of transcripts under stress conditions was >10 times higher in the most efficient cultivar Crac (Fig. 5b). The same behaviour was observed for *TaPHO2* under Pi limitation. Here, an increase of 6- and 2-fold was observed for Crac and Tukan, respectively, resulting in almost 5-fold higher transcript levels in Crac (Fig. 5c). We further assessed the expression of the three *TaPHO2* alleles present in the wheat genome (1A, 1B, and 1D), using specific primers (Supplementary Table S2). Different patterns were observed for the three alleles regarding P responses (Supplementary Fig. S3a–c). Overall, Crac *TaPHO2* alleles presented a higher induction in Pi starvation, especially *TaPHO2* 1B, with an increase of 25-fold. Tukan *TaPHO2* 1B and 1D showed a small, but significant increase in its expression under Pi deprivation (2.8- and 2-fold, respectively), while no differences were observed for *TaPHO2* 1A expression. No differences in gene expression were observed for the transporter *TaPHO1* (Fig. 5d).

In order to assess the dynamics of Pi signalling in the two cultivars, a time-course experiment was performed under the same conditions as described before, but harvesting plants after 2, 4, and 7 d of Pi deprivation. Interestingly, Crac presented an induction of *TaPHO2*, *TaIPS1*, and tae-miR399b from day 2, which was steadily increased over time. However, in Tukan, the increasing response of these genes to Pi starvation was only observed at day 7 (Fig. 6), indicating a faster response by Crac to Pi deprivation.

Strigolactone levels in Crac and Tukan

Since the root architecture of Crac and Tukan was different under Pi starvation, we assessed whether SLs were involved in such changes. We first performed a germination bioassay with *P. ramosa* seeds using root extracts from the two cultivars. GR24 (10^{-8} M and 10^{-9} M), used as positive control, induced high germination, while water (negative control) did not induce any germination. Under Pi-sufficient conditions, Crac induced twice the germination of *P. ramosa* comparted

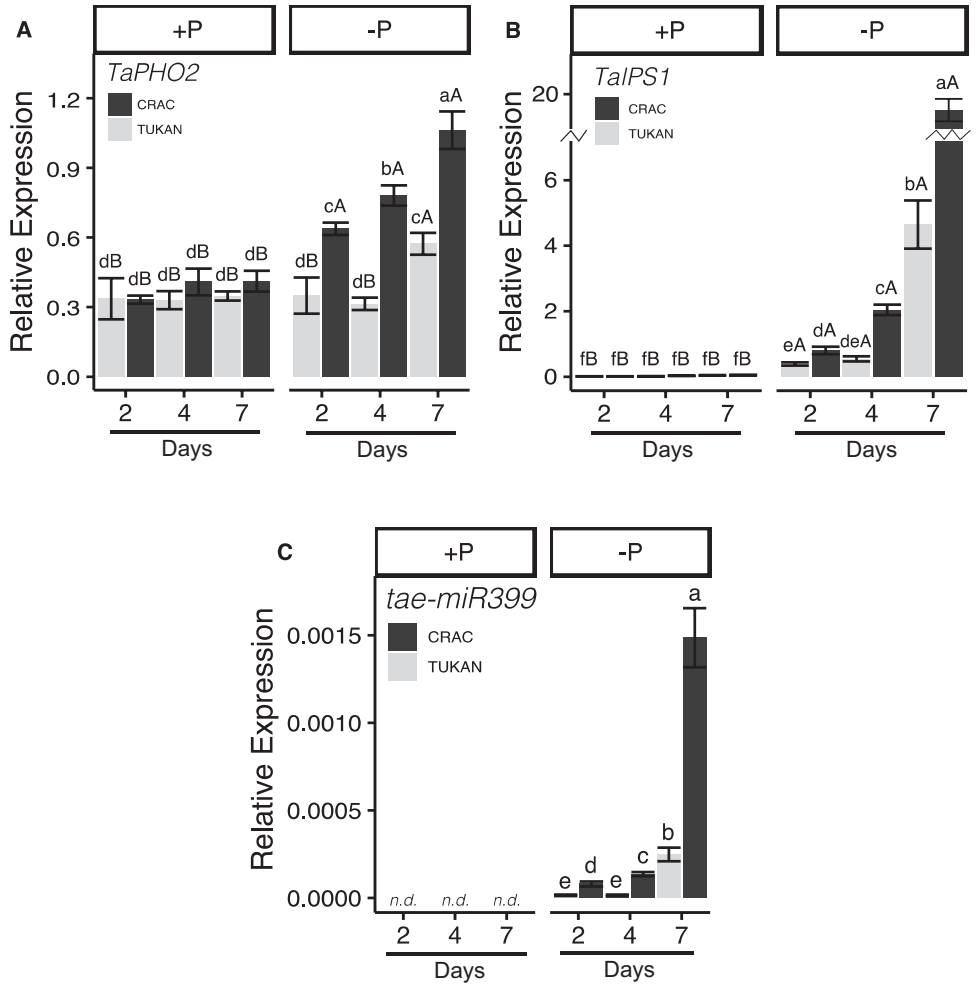

Fig. 6. Expression levels of genes involved in P signalling and homeostasis in roots of Crac (dark bars) and Tukan (light bars) plants grown in nutrient solution with Pi (+P; 150 µM) and without Pi (–P) harvested after 2, 4, and 7 d of Pi deprivation. Graphics represent the expression of genes *TaPHO2*, *TaIPS1*, and tae-miR399. Expression levels were referenced to the expression of the housekeeping gene *TahnRNPQ*. Bars represent the means of five independent replicates (±SE). Lower case letters indicate differences between cultivars in the same condition, and upper case letters indicate differences within the same cultivar and day between +P and –P conditions, as determined by Student's *t*-test ($P<0.05$). n.d, non-detected.

with Tukan (Fig. 7a), suggesting a higher basal level of SLs in that cultivar. Pi starvation increased germination in both cultivars: 7% and 10% for Crac and Tukan, respectively (Fig. 7a). Orobanchol was detected in the root extracts of both cultivars. This SL was reported as the main SL present in wheat exudates (Yoneyama *et al.*, 2012). Orobanchol levels were significantly increased ~80% in Crac plants subjected to Pi starvation ($P<0.01$; Fig. 7b). This stress also increased the amount of orobanchol in Tukan, which was not detected under Pi-sufficient conditions. Here, orobanchol levels under Pi deficiency were similar to those in Crac in the absence of stress, indicating lower levels of SLs in Tukan, as previously observed in the *P. ramosa* germination bioassays (Fig. 7a). In addition to orobanchol, the SL fabacyl acetate was also detected in trace amounts in some samples. It was only detected in extracts from plants grown under Pi limitation, indicating that its biosynthesis was also promoted by Pi starvation, and also showing higher contents in Crac (data not shown).

To explore whether the elevated SL levels are related to a higher activity of the SL biosynthetic pathway in the Crac cultivar, the expression of two key genes involved in SL biosynthesis—*TaD27,* and *TaCCD8*—was analysed. The sequential action of these two enzymes gives rise to carlactone, the precursor of all the canonical SLs, including strigol- and orobanchol-type SLs (Al-Babili and Bouwmeester, 2015; Zhang *et al.*, 2018). The search for the wheat *D27* gene was conducted using BLAST against its orthologue sequence from rice (LOC107276001). Two complete sequences were found for copies in chromosomes 7A and 7D (accession numbers: KX168420.1 and KX168421.1), showing 52% and 54% homology, respectively, with rice *D27* (Supplementary Fig. S4). The same strategy was applied for *CCD8*; however, no direct match was found. Therefore, the sequence encoding the putative wheat *CCD8* was searched in the wheat genome database (IWGSC database), using BLAST against its orthologue sequence from *Zea mays* (*ZmCCD8*). One sequence for each chromosome was found (3A, 3B, and 3D) (Supplementary Fig. S5). The sequences obtained for *TaD27* and *TaCCD8* were checked for the presence of the functional domain DUF4033 and RPE65, respectively, and their homology with wheat close relatives was assessed (Supplementary Figs S4a, S5b). Specific primers for *TaD27* and *TaCCD8* were designed to perform

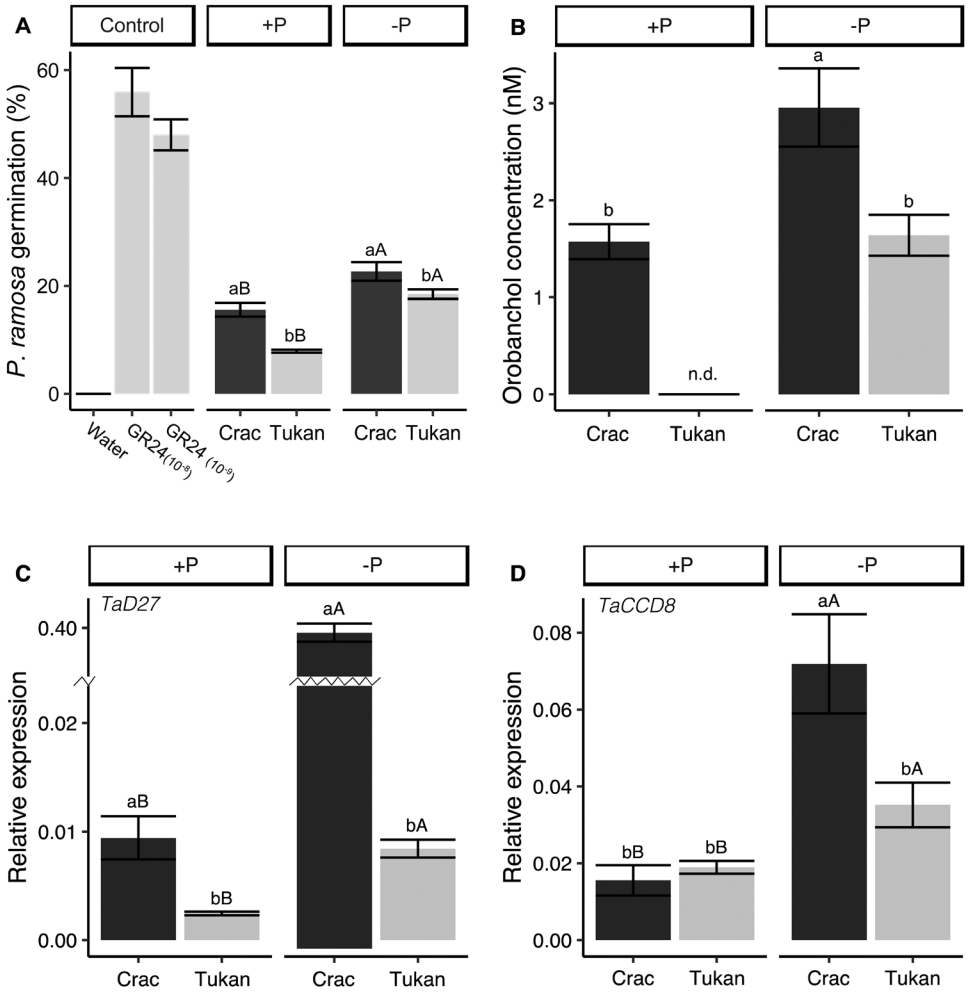

Fig. 7. Analysis of SL levels in roots of Crac and Tukan plants grown in nutrient solution with Pi (+P; 150 µM) and without Pi for the last week (–P) harvested at Zadoks growth stage 24 (Zadoks *et al.*, 1974). (A) Germination of *P. ramosa* seeds induced by extracts from Crac (dark bars) and Tukan (light bars). (B) Orobanchol levels in root extracts determined by UHPLC-MS-MS. Data represent the means of three independent replicates (±SE). Different letters indicate significant differences between means, as determined by Tukey LSD test analysis. n.d, not detected. Expression levels of two SL biosynthesis genes: (C) *TaD27* and (D) *TaCCD8*. Bars represent the means of five independent replicates (±SE). Lower case letters indicate differences between cultivars in the same condition, and upper case letters indicate differences within the same cultivar under normal and deficient Pi conditions, as determined by Student's *t*-test ($P<0.05$).

qPCR (Supplementary Table S1). The basal expression of *TaD27* under Pi-sufficient conditions was almost 4-fold higher in Crac roots than in Tukan (Fig. 7c). However, no differences in basal expression levels of *TaCCD8* were found between the two cultivars (Fig. 7d). Pi deprivation induced *TaD27* transcript levels ~40-fold in Crac, but only 3-fold in Tukan (Fig. 7c). A similar trend was observed for *TaCCD8*, with an increase in the expression levels of ~5-fold in Crac and only ~2-fold in Tukan (Fig. 7d). These results confirm that Crac produces higher basal levels of SLs than Tukan, and responds more efficiently to P starvation through a stronger promotion of SL biosynthesis, which would favour a greater and faster development of the root system in response to Pi-limiting conditions.

Discussion

Crac has an improved root system development and a higher Pi acquisition capacity

In the present work, we analysed the physiological and molecular traits of two commercial wheat cultivars—Crac and Tukan—showing differential PAE under Pi-limiting conditions (Seguel *et al.*, 2017). Interestingly, under that stress condition, yield parameters correlated with root biomass and Pi acquisition (Seguel *et al.*, 2017). Here, when plants were grown under Pi-sufficient conditions, no differences in Pi acquisition and biomass production/partitioning were observed, highlighting that the differences further discussed are specifically related to contrasting responses to Pi limitation. In this sense, our results are in agreement with a previous study in plants grown in an acidic high Pi-fixing soil (Seguel *et al.*, 2017). We show that Crac also presents a higher Pi accumulation in shoots and roots when subjected to Pi deprivation (Table 1). Alterations in shoot and root growth and/or architecture are the most widespread plant adaptations to Pi starvation, affecting the root:shoot ratio (Haling *et al.*, 2016; Chien *et al.*, 2018). Interestingly, under these conditions, Crac showed smaller losses of shoot biomass production and greater increments in root growth, giving rise to higher root:shoot ratios, which correlated with total Pi acquisition in all experiments. In addition to greater root:shoot ratios, Crac showed larger and thinner roots than Tukan (Supplementary Figs S2, S6).

Altogether, these phenotypic differences would allow Crac to have a higher soil exploration capacity in search of Pi patches under limiting conditions.

Improved PAE is associated with higher expression of PHT1 *Pi transporter genes*

Several studies correlate higher Pi accumulation and, in most cases, plant growth with higher expression of Pi transporters of the *PHT1* family (Liu *et al.*, 2013; Wang *et al.*, 2013; Ham *et al.*, 2018). Recently, it has been shown that under Pi starvation, transcript levels of the gene *TaPht1;2* were the most abundant of all the *PHT1* transporter geness described in wheat (Grün *et al.*, 2017). This transporter is the orthologue of the rice *OsPht1;2*, which is also highly expressed in Pi-deprived roots, and it is characterized as a low-affinity Pi transporter, mainly involved in internal Pi translocation (Ai *et al.*, 2009). The other Pi transporter gene analysed was *TaPht1;10*, whose expression levels were lower (~25-fold) than those of *TaPht1;2*. *TaPht1;10* and its orthologues in rice—*OsPht1;9* and *OsPht1.10*—are considered as high-affinity Pi transporters, and are mainly induced under long-term Pi starvation (Ai *et al.*, 2009; Grün *et al.*, 2017). As expected, both genes were highly induced by Pi deficiency in both cultivars, confirming their role in Pi uptake and distribution under nutritional stress. In agreement with this, it has been shown that transgenic *Nicotiana tabacum* plants overexpressing a *Pht1;2* gene displayed a higher Pi content and better growth than the corresponding wild type (Cao *et al.*, 2018). These plants also showed enhanced Pi in the xylem sap, indicating that this transporter is involved in root:shoot Pi translocation. No differences in gene expression were observed for *TaPHO1*, a component of the other family of Pi transporters and involved in Pi xylem loading (Franco-Zorrilla *et al.*, 2007). However, this was not surprising since it was previously shown that this transporter is regulated post-transcriptionally by the action of *PHO2* (Fig. 1) (Lin *et al.*, 2008; Huang *et al.*, 2013). Notably, basal levels of the two genes encoding *PHT1* transporters under sufficient Pi conditions were higher in the most efficient cultivar Crac, and the final levels under Pi starvation were much higher than in Tukan (Fig. 4). In this sense, these differences could be related to the internal SL levels, which are directly linked to *PHT1* expression and other PSI genes in Arabidopsis (Ito *et al.*, 2015). These results, together with the enhanced root system of Crac, indicate that this cultivar is better suited to respond readily to this type of nutritional stress by an improved Pi uptake and root:shoot translocation capacity.

P signalling and homeostasis, and its relationship to SLs

It is generally accepted that *PHO2* activity is rapidly reduced under Pi deficiency due to high induction of miR399 in the first hours of stress, which overcomes protection by *IPS1* (Ajmera *et al.*, 2018). However, there are only a few studies evaluating the effect of long-term Pi deprivation on the regulation of this pathway. In a time-course study in rice, Ajmera *et al.* (2018) found that the number of *IPS1* transcripts increased slowly, but more strongly than those of miR399, leading to a relative increase of *PHO2* levels after 1 week of stress. A similar pattern was observed in barley plants after 16 d of Pi starvation, where cultivars showing high levels of *HvIPS2* matched with those with higher *HvPHO2* expression (Huang *et al.*, 2011). In the present study, an induction of tae-miR399b was observed after 1 week of Pi deficiency. However, the total number of transcripts at this time point was much lower than those of *TaIPS1* (>1000 times), leading to a complete sequestration of tae-miR399 transcripts. This blockage would explain the high induction of *TaPHO2* observed in our system (Fig. 5). *Arabidopsis thaliana IPS1*-overexpressing lines also presented a enhanced *PHO2* accumulation due to higher *IPS1*-mediated miR399 sequestration (Franco-Zorrilla *et al.*, 2007). Therefore, it seems that the regulation of P signalling and homeostasis by the triad *IPS1*–miR399–*PHO2* is dynamic, showing a different regulation over time. Based on the responses observed in wheat seedlings and other model plants at different developmental stages (Huang *et al.*, 2011; Ouyang *et al.*, 2016; Ajmera *et al.*, 2018), we propose a model to explain the behaviour of these three regulators during early and late responses upon Pi starvation (Fig. 8). According to this, during the first hours of stress, there might be a rapid induction of miR399 levels, which mediates the cleavage of *PHO2* transcripts, probably to increase the relative amount of *PHT1* members to promote Pi uptake from the soil, with the corresponding translocation to the shoots. In the case where Pi limitation continues over time, transcripts of *IPS1* would increase greatly to lock miR399, and probably to exert other regulatory functions as well, with the concomitant increase in *PHO2* levels. This increase will trigger late Pi responses related to the improvement of Pi uptake and modification of root architecture, probably to search for new Pi 'hotspots', among others. In agreement with this hypothesis, higher *PHO2* levels under Pi starvation in barley correlated

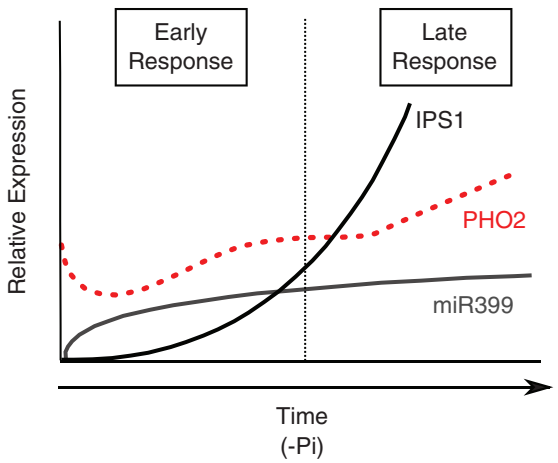

Fig. 8. Proposed model for the regulation of P signalling and homeostasis by the module *IPS1*–miR399–*PHO2*. At early stages of Pi starvation, the high miR399 induction favours *PHO2* transcript degradation and triggers early phosphate starvation responses (PSRs). As Pi starvation follows, the miR399:*IPS1* ratio diminishes due to sustained high expression of *IPS1*, increasing *PHO2* degradation, and initiating late PSRs. Black and grey lines represent *IPS1* and miR399 expression, respectively, and the dotted line represent *PHO2* expression. (This figure is available in colour at *JXB* online.)

with a higher root:shoot ratio (Huang *et al.*, 2011). Conversely, wheat plants blocked at *TaPHO2* showed a lower root:shoot ratio (Ouyang *et al.*, 2016). The initial down-regulation of *PHO2* proposed in our model was not observed in the time-course experiment, probably because this regulation may occur within hours after Pi deprivation at this developmental stage. On the other hand, the *IPS1*–miR399 relationship did not fully explain the variation in *PHO2* levels, which was in accordance with the responses observed in rice (Ajmera *et al.*, 2018). We suggest two possibilities to explain this fact: (i) there must be more genes involved in this complex regulation; and/or (ii) when *IPS1* transcripts reach a certain level, they are sufficient to sequester miR399. Thus, further increases of these transcripts would not affect *PHO2* degradation. Further studies are required to fully decipher how this signalling and homeostasis pathway works, especially under longer periods of Pi starvation and at different plant developmental stages.

As for the *TaPht1;2* and *TaPht1;10* transporters, the levels of the three regulators *IPS1*–miR399b–*PHO2* under Pi limitation were much higher in the cultivar Crac, with enhanced PAE, than in the less efficient cultivar Tukan. However, the basal transcript levels of these genes were similar under P-sufficient conditions. Again, these results show that Crac is more efficient in the response to Pi deficiency, and that this enhanced efficiency is due to a better and faster Pi starvation signalling and homeostasis regulation. In agreement with this, Crac showed higher basal levels of SLs than Tukan (Fig. 6). SLs, together with other phytohormones, are involved in the regulation of P homeostasis under Pi limitation by modulating P signalling-associated pathways and root development (Waters *et al.*, 2017; Chien *et al.*, 2018). Therefore, it might be the case that the higher SL levels in Crac would act as a priming signal under Pi starvation to boost plant responses to the stress. However, further research is needed to clarify the connection between SLs and P signalling.

Understanding the physiological mechanisms of improved PAE and the genetic basis therein will allow breeders to select more P-efficient cultivars. This knowledge will help to diminish the use of P fertilizers in agriculture, thus reducing costs and alleviating the excessive consumption of this non-renewable resource. However, traits associated with PAE are complex and context dependent. In the present study, we suggest that the higher PAE of the commercial cultivar Crac might be related to the SLs–P signalling relationship and homeostasis through fine-tuning modulation of *PHO2* activity. This modulation, in the long term, would relatively reduce shoot Pi loading, favouring the development of an enhanced root system and giving rise to an increased soil exploration capacity in search of Pi patches under limiting conditions and to increase Pi acquisition in high Pi-fixing soils. Further research is needed to fully understand the SLs–P signalling relationship to develop new strategies for improved plant performance under P stress conditions.

Supplementary data

Supplementary data are available at *JXB* online.

Table S1. Selected chemical properties of the soil used in the rhizobox experiment.

Table S2. Primer sequences used in the qPCR analysis.

Table S3. Effects (%) of Pi starvation on plants grown in hydroponics.

Fig. S1. Example of the different experimental conditions.

Fig. S2. Main results of the effects of Pi starvation in the rhizobox experiment.

Fig. S3. Expression levels of *TaPHO2* alleles.

Fig. S4. Phylogenetic analysis of *D27* sequences and amino acid sequences.

Fig. S5. Phylogenetic analysis of partial *CCD8* sequences and amino acid sequences.

Fig. S6. Example of Crac and Tukan root systems.

Acknowledgements

This work was supported by funding from FONDECYT grants 11160385 and 1170264 from Comisión Nacional de Investigación Científica y Tecnológica (CONICYT-Chile), CONICYT DOCTORADO NACIONAL 2016 (21161474), CONICYT+PAI/CONCURSO NACIONAL TESIS DE DOCTORADO EN EL SECTOR PRODUCTIVO 2017 (T7817120011), CONICYT/FONDAP/15130015, and AGL2015-64990-C2-1R (MINECO-Spain). We also acknowledge Dr Koichi Yoneyama and Dr Xiaoan Xie for kindly providing the natural strigolactones used to set up their analytical quantification, Dr Gustavo Curaqueo for the analysis of the root scanning system, Campex Baer® for their agronomical support, BIOREN-UFRO for providing their facilities, and Dr María J. Pozo and Dr Francisco Macías for critical reading of the manuscript and support.

References

Ai P, Sun S, Zhao J, *et al*. 2009. Two rice phosphate transporters, OsPht1;2 and OsPht1;6, have different functions and kinetic properties in uptake and translocation. The Plant Journal **57**, 798–809.

Ajmera I, Shi J, Giri J, Wu P, Stekel DJ, Lu C, Hodgman TC. 2018. Regulatory feedback response mechanisms to phosphate starvation in rice. NPJ Systems Biology and Applications **4**, 4.

Al-Babili S, Bouwmeester HJ. 2015. Strigolactones, a novel carotenoid-derived plant hormone. Annual Review of Plant Biology **66**, 161–186.

Bennett EM, Carpenter SR, Caraco NF. 2001. Human impact on erodable phosphorus and eutrophication: a global perspective. BioScience **51**, 227–234.

Bouwmeester HJ, Roux C, Lopez-Raez JA, Bécard G. 2007. Rhizosphere communication of plants, parasitic plants and AM fungi. Trends in Plant Science **12**, 224–230.

Bovill W, Huang C, Mcdonald G. 2013. Genetic approaches to enhancing phosphorus-use efficiency (PUE) in crops: challenges and directions. Crop & Pasture Science **64**, 179–198.

Campos P, Borie F, Cornejo P, López-Ráez JA, López-García Á, Seguel A. 2018. Phosphorus acquisition efficiency related to root traits: is mycorrhizal symbiosis a key factor to wheat and barley cropping? Frontiers in Plant Science **9**, 752.

Cao Y, Sun D, Chen JX, Mei H, Ai H, Xu G, Chen Y, Ma LQ. 2018. Phosphate transporter PvPht1;2 enhances phosphorus accumulation and plant growth without impacting arsenic uptake in plants. Environmental Science & Technology **52**, 3975–3981.

Chien P-S, Chiang C-P, Leong SJ, Chiou T-J. 2018. Sensing and signaling of phosphate starvation: from local to long distance. Plant & Cell Physiology **59**, 1714–1722.

Cordell D, Drangert JO, White S. 2009. The story of phosphorus: global food security and food for thought. Global Environmental Change **19**, 292–305.

Ericsson T. 1995. Growth and shoot:root ratio of seedlings in relation to nutrient availability. Plant and Soil **168**, 205–214.

Franco-Zorrilla JM, Valli A, Todesco M, Mateos I, Puga MI, Rubio-Somoza I, Leyva A, Weigel D, García JA, Paz-Ares J. 2007. Target mimicry provides a new mechanism for regulation of microRNA activity. Nature Genetics **39**, 1033–1037.

Grün A, Buchner P, Broadley MR, Hawkesford MJ. 2017. Identification and expression profiling of Pht1 phosphate transporters in wheat in controlled environments and in the field. Plant Biology **20**, 374–389.

Haling RE, Yang Z, Shadwell N, Culvenor RA, Stefanski A, Ryan MH, Sandral GA, Kidd DR, Lambers H, Simpson RJ. 2016. Root morphological traits that determine phosphorus-acquisition efficiency and critical external phosphorus requirement in pasture species. Functional Plant Biology **43**, 815–826.

Ham BK, Chen J, Yan Y, Lucas WJ. 2018. Insights into plant phosphate sensing and signaling. Current Opinion in Biotechnology **49**, 1–9.

Hargreaves CE, Gregory PJ, Bengough AG. 2009. Measuring root traits in barley (*Hordeum vulgare* ssp. *vulgare* and ssp. *spontaneum*) seedlings using gel chambers, soil sacs and X-ray microtomography. Plant and Soil **316**, 285–297.

Heffer P. 2013. Assessment of fertilizer use by crop at the global level. Paris: International Fertilizer Industry Association.

Hewitt EJ. 1966. Sand and water culture methods used in the study of plant nutrition. Maidstone, UK: Commonwealth Bureau of Horticulture and Plantation Crops.

Huang CY, Shirley N, Genc Y, Shi B, Langridge P. 2011. Phosphate utilization efficiency correlates with expression of low-affinity phosphate transporters and noncoding RNA, IPS1, in barley. Plant Physiology **156**, 1217–1229.

Huang TK, Han CL, Lin SI, *et al*. 2013. Identification of downstream components of ubiquitin-conjugating enzyme PHOSPHATE2 by quantitative membrane proteomics in Arabidopsis roots. The Plant Cell **25**, 4044–4060.

Ito S, Nozoye T, Sasaki E, *et al*. 2015. Strigolactone regulates anthocyanin accumulation, acid phosphatases production and plant growth under low phosphate condition in Arabidopsis. PLoS One **10**, e0119724.

Lambers H, Martinoia E, Renton M. 2015. Plant adaptations to severely phosphorus-impoverished soils. Current Opinion in Plant Biology **25**, 23–31.

Lan P, Li W, Schmidt W. 2015. 'Omics' approaches towards understanding plant phosphorus acquisition and use. Annual Plant Reviews **48**, 65–98.

Lin SI, Chiang SF, Lin WY, Chen JW, Tseng CY, Wu PC, Chiou TJ. 2008. Regulatory network of microRNA399 and PHO2 by systemic signaling. Plant Physiology **147**, 732–746.

Liu TY, Huang TK, Tseng CY, Lai YS, Lin SI, Lin WY, Chen JW, Chiou TJ. 2012. PHO2-dependent degradation of PHO1 modulates phosphate homeostasis in Arabidopsis. The Plant Cell **24**, 2168–2183.

Liu X, Zhao X, Zhang L, Lu W, Li X, Xiao K. 2013. TaPht1;4, a high-affinity phosphate transporter gene in wheat (*Triticum aestivum*), plays an important role in plant phosphate acquisition under phosphorus deprivation. Functional Plant Biology **40**, 329–341.

López-Arredondo DL, Leyva-González MA, González-Morales SI, López-Bucio J, Herrera-Estrella L. 2014. Phosphate nutrition: improving low-phosphate tolerance in crops. Annual Review of Plant Biology **65**, 95–123.

López-Ráez JA, Charnikhova T, Gómez-Roldán V, *et al*. 2008. Tomato strigolactones are derived from carotenoids and their biosynthesis is promoted by phosphate starvation. New Phytologist **178**, 863–874.

López-Ráez JA, Shirasu K, Foo E. 2017. Strigolactones in plant interactions with beneficial and detrimental organisms: the Yin and Yang. Trends in Plant Science **22**, 527–537.

Murphy J, Riley JP. 1962. A modified single solution method for the determination of phosphate in natural waters. Analytica Chimica Acta **27**, 31–36.

Ouyang X, Hong X, Zhao X, Zhang W, He X, Ma W, Teng W, Tong Y. 2016. Knock out of the PHOSPHATE 2 gene *TaPHO2-A1* improves phosphorus uptake and grain yield under low phosphorus conditions in common wheat. Scientific Reports **6**, 29850.

Pant BD, Buhtz A, Kehr J, Scheible WR. 2008. MicroRNA399 is a long-distance signal for the regulation of plant phosphate homeostasis. The Plant Journal **53**, 731–738.

Puga MI, Rojas-Triana M, de Lorenzo L, Leyva A, Rubio V, Paz-Ares J. 2017. Novel signals in the regulation of Pi starvation responses in plants: facts and promises. Current Opinion in Plant Biology **39**, 40–49.

Rial C, Varela RM, Molinillo JMG, López-Ráez JA, Macías FA. 2019. A new UHPLC-MS/MS method for the direct determination of strigolactones in root exudates and extracts. Phytochemical Analysis **30**, 110–116.

Rose TJ, Wissuwa M. 2012. Rethinking internal phosphorus utilization efficiency; a new approach is needed to improve PUE in grain crops. Advances in Agronomy **116**, 185–217.

Rubio V, Linhares F, Solano R, Martín AC, Iglesias J, Leyva A, Paz-Ares J. 2001. A conserved MYB transcription factor involved in phosphate starvation signaling both in vascular plants and in unicellular algae. Genes & Development **15**, 2122–2133.

Scheible W-R, Rojas-Triana M. 2015. Sensing, signalling, and control of phosphate starvation in plants: molecular players and applications. Annual Plant Reviews **48**, 23–63.

Seguel A, Cornejo P, Ramos A, Von Baer E, Cumming J, Borie F. 2017. Phosphorus acquisition by three wheat cultivars contrasting in aluminium tolerance growing in an aluminium-rich volcanic soil. Crop and Pasture Science **68**, 305–316.

Syers J, Johnston A, Curtin D. 2008. Efficiency of soil and fertilizer phosphorus use: reconciling changing concepts of soil phosphorus behaviour with agronomic information. Rome: FAO.

Taylor GJ, Foy CD. 1985. Mechanisms of aluminum tolerance in *Triticum aestivum* L. (wheat). I. Differential pH induced by winter cultivars in nutrient solutions. American Journal of Botany **72**, 695–701.

Teng W, Zhao Y-Y, Zhao X-Q, He X, Ma W-Y, Deng Y, Chen X-P, Tong Y-P. 2017. Genome-wide identification, characterization, and expression analysis of PHT1 phosphate transporters in wheat. Frontiers in Plant Science **8**, 543.

Ulrich AE, Frossard E. 2014. On the history of a reoccurring concept: phosphorus scarcity. The Science of the Total Environment **490**, 694–707.

van de Wiel CCM, van der Linden CG, Scholten OE. 2016. Improving phosphorus use efficiency in agriculture: opportunities for breeding. Euphytica **207**, 1–22.

Wang J, Sun J, Miao J, *et al*. 2013. A phosphate starvation response regulator Ta-PHR1 is involved in phosphate signalling and increases grain yield in wheat. Annals of Botany **111**, 1139–1153.

Waters MT, Gutjahr C, Bennett T, Nelson DC. 2017. Strigolactone signaling and evolution. Annual Review of Plant Biology **68**, 291–322.

Wissuwa M, Ae N, Jones SS. 2001. Genotypic variation for tolerance to phosphorus deficiency in rice and the potential for its exploitation in rice improvement. Plant Breeding **120**, 43–48.

Xu Y, Liu F, Han G, Cheng B. 2018. Genome-wide identification and comparative analysis of phosphate starvation-responsive transcription factors in maize and three other gramineous plants. Plant Cell Reports **37**, 711–726.

Yao Q, Wang LR, Zhu HH, Chen JZ. 2009. Effect of arbuscular mycorrhizal fungal inoculation on root system architecture of trifoliate orange (*Poncirus trifoliata* L. Raf.) seedlings. Scientia Horticulturae **121**, 458–461.

Yoneyama K, Xie X, Kim HI, Kisugi T, Nomura T, Sekimoto H, Yokota T, Yoneyama K. 2012. How do nitrogen and phosphorus deficiencies affect strigolactone production and exudation? Planta **235**, 1197–1207.

Yoneyama K, Xie X, Kusumoto D, Sekimoto H, Sugimoto Y, Takeuchi Y, Yoneyama K. 2007. Nitrogen deficiency as well as phosphorus deficiency in sorghum promotes the production and exudation of 5-deoxystrigol, the host recognition signal for arbuscular mycorrhizal fungi and root parasites. Planta **227**, 125–132.

Zadoks JC, Chang TT, Konzak CF. 1974. A decimal code for the growth stages of cereals. Weed Research **14**, 415–421.

Zhang Y, Lv S, Wang G. 2018. Strigolactones are common regulators in induction of stomatal closure in planta. Plant Signaling & Behavior **13**, e1444322.

Zhou J, Jiao F, Wu Z, Li Y, Wang X, He X, Zhong W, Wu P. 2008. OsPHR2 is involved in phosphate-starvation signaling and excessive phosphate accumulation in shoots of plants. Plant Physiology **146**, 1673–1686.

Zhu J, Ingram PA, Benfey PN, Elich T. 2011. From lab to field, new approaches to phenotyping root system architecture. Current Opinion in Plant Biology **14**, 310–317.